Turk J Phys
31 (2007) , 11 – 29.

Physical Properties of $(Li_2O)_{0.40}(Fe_2O_3)_{0.05-x}$ $(P_2O_5)_{0.55}$: $(Ag_2O)_x$ Glasses

K. Sambasiva RAO, N. Krishna MOHAN and N. VEERAIAH
Department of Physics, Acharya Nagarjuna University PG Centre, Nuzvid 521 201-INDIA
e-mail: nvr8@rediffmail.com

Received 08.12.2006

Abstract

Li_2O–Fe_2O_3–P_2O_5 glasses containing small concentrations of Ag_2O from 0 to 2 mol% were prepared. Samples are characterized by X-ray diffraction and scanning electron microscope techniques. A number of studies viz., chemical durability, dielectric studies (constant ε', loss tan δ, a.c. conductivity σ_{ac} over a range of frequency and temperature), spectroscopic (infrared, optical absorption ESR spectra) and magnetic susceptibility studies of these glasses, have been carried out. The interesting variations observed in all these properties with the concentration of Ag^+ ions have been analyzed in the light of different oxidation states and environment of iron ions in the glass network.

Key Words: Glasses, dielectrics, optical materials and properties.

1. Introduction

Iron phosphate glasses are known for their high chemical durability and for their application in vitrifying nuclear waste [1, 2]. With the addition of lighter alkali ion-like lithium, iron phosphate glasses becomes suitable for a variety of technological applications such as solid electrolytes, and in electrochemical devices such as high energy density batteries [3]. Mixing of silver oxide in small quantity to phosphate glasses presents an added advantage allowing these glasses to be used as super ionic solids [4]. Mixed electronic and ionic, pure electronic or pure ionic conduction is expected in these glasses, depending upon the constituent composition of the glass. The materials that exhibit mixed conduction mechanism find numerous applications, such as cathodes in electro chemical cells, in smart windows etc. [5]. Electronic conduction in such materials is predicted due to polaron hopping, where the ionic conduction is expected due to the diffusion of alkali or other dopant ions such as silver. Phosphorous pentoxide is a strong glass network forming oxide, participating in the network with PO_4 structural units. One of the four oxygen atoms in PO_4 tetrahedron is doubly bonded to the phosphorus atom with the substantial π-bond character to account for pentavalency of phosphorous. The PO_4 tetrahedrons are linked together with covalent bonding in chains or rings by bridging oxygens. Neighbouring phosphate chains are linked together by cross bonding between the metal cation and two non-bridging oxygen atoms of each PO_4 tetrahedron in general, the P–O–P bond between PO_4tetrahedra is much stronger than the cross bond between chains via the metal cations [6]. Iron ions are expected to exist mainly in Fe^{3+} state in Li_2O–Fe_2O_3–P_2O_5 glass network.

However, regardless of the oxidation state of the iron in the starting glass batch, the final glass contains both Fe^{3+} and Fe^{2+} ions [7]. The concentration of Fe^{2+} (or Fe^{3+}) in these iron phosphate glasses depends

primarily upon the melting temperature, and to some extent on the melting time. Majority of the studies available on iron phosphate glasses are on Mossbauer spectra [8, 9]. The studies on dielectric properties viz., dielectric constant, loss and a.c. conductivity (over a wide range of frequency and temperature) not only help understand the a.c. conduction mechanism but also contribute additional information on structural aspects of the glasses. Work along these lines has been carried out in recent years on a variety of inorganic glass systems yielding valuable information [10, 11]. However, such type of studies on iron phosphate glasses, especially those mixed with silver ions, are very few.

The intent of the present study is to report the results of a systematic study on dielectric properties, e.g. dielectric constant, loss and a.c. conductivity (over a wide range of frequency and temperature) and breakdown strength in air medium at room temperature of Li_2O–Fe_2O_3–P_2O_5 glasses doped with small concentrations of Ag_2O, and to throw some light on the influence of Ag^+ ion on structural properties these glasses using the results of these studies with the aid of the data on IR, ESR and optical absorption and magnetic susceptibility. Studies on chemical durability are also included.

2. Experimental Methods

Within the glass forming region of Li_2O–Fe_2O_3–P_2O_5 glass system, the following compositions with a gradual increase in the concentration of Ag_2O, are chosen for the present study:

FA_0: $(Li_2O)_{0.40}(Fe_2O_3)_{0.050}(P_2O_5)_{0.55}$

FA_2: $(Li_2O)_{0.40}(Fe_2O_3)_{0.048}(P_2O_5)_{0.55}$: $(Ag_2O)_{0.002}$,

FA_4: $(Li_2O)_{0.40}(Fe_2O_3)_{0.046}(P_2O_5)_{0.55}$: $(Ag_2O)_{0.004}$,

FA_6: $(Li_2O)_{0.40}(Fe_2O_3)_{0.044}(P_2O_5)_{0.55}$: $(Ag_2O)_{0.006}$,

FA_8: $(Li_2O)_{0.40}(Fe_2O_3)_{0.042}(P_2O_5)_{0.55}$: $(Ag_2O)_{0.008}$,

FA_{10}: $(Li_2O)_{0.40}(Fe_2O_3)_{0.040}(P_2O_5)_{0.55}$: $(Ag_2O)_{0.010}$,

FA_{15}: $(Li_2O)_{0.40}(Fe_2O_3)_{0.035}(P_2O_5)_{0.55}$: $(Ag_2O)_{0.015}$,

FA_{20}: $(Li_2O)_{0.40}(Fe_2O_3)_{0.030}(P_2O_5)_{0.55}$: $(Ag_2O)_{0.020}$.

Appropriate amounts of "analar" grade reagents of Li_2CO_3, $(NH_4)H_2PO_4$, Fe_2O_3 and Ag_2O were thoroughly mixed in an agate mortar and melted in a thick walled platinum crucible at 1100 ± 10 °C for about 1 h until a bubble-free liquid was formed. The resultant melt was then cast in a brass mould and subsequently annealed at 350 °C. X-ray diffraction (Figure 1) and scanning electron microscopy studies were used to confirm that the samples prepared were vitreous. The results of these studies clearly indicated that the samples prepared are free from crystalline phases.

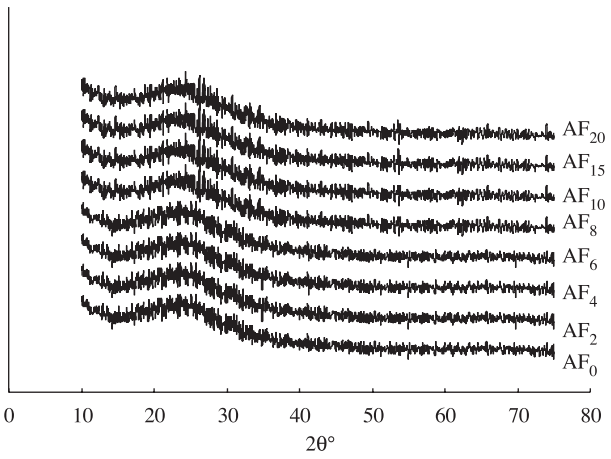

Figure 1. XRD patterns of Li_2O–P_2O_5–Fe_2O_3 glasses containing different concentrations of Ag2O.

The density d of the glasses was determined to an accuracy of (±0.001) by the standard principle of Archimedes' using o-xylene (99.99% pure) as the buoyant liquid. The mass of the samples was measured to an accuracy of 0.1 mg using a Denver balance, model APX-200. For evaluating the chemical durability, the bulk glasses were suspended by a weightless strand in about 100 ml of water of pH 7 for about 4 h at 90 °C for about 12, 24, 48 hours. At each time interval the weight loss (ΔW) is evaluated and the dissolution rate DR for the bulk glasses were calculated using the relation $DR = \Delta W$ / (St) g/cm^2/min, where S is the surface area of the sample and t is the time of immersion.

The glasses were then ground and optically polished. The final dimensions of the glasses used for electrical and optical absorption measurements were about 1 ×1 × 0.2 cm^3. The glass transition temperature of these glasses were determined by differential scanning calorimetric studies using a TA instruments model DSC-2010 with a programmed heating rate of 10 °C·min^{-1}, in the temperature range 30–550 °C.

The optical absorption spectra of the glasses were recorded at room temperature in the wavelength range 300–800 nm up to a resolution of 0.1 nm using Cary-5000 spectrophotometer. The electron spin resonance (ESR) spectra of the fine powders of the samples were recorded at liquid nitrogen temperature on Jeol JES-TES100 X-band EPR spectrometer.

Infrared transmission spectra were recorded on a Jasco FT/IR–5300 spectrophotometer with a resolution of 0.1 cm^{-1} in the range 400–2000 cm^{-1} using potassium bromide pellets (300 mg) containing pulverized sample (1.5 mg). These pellets were pressed in a vacuum die at ∼680 MPa. A thin layer of silver paint was applied on either side of the large-faces of the samples, in order to serve as electrodes for dielectric measurements. The dielectric measurements were made on LCR Meter (Hewlett-Packard Model-4263 B) in the frequency range 10^2–10^5 Hz and in the temperature range 30–250 °C. The accuracy in the measurement of dielectric constant is ∼0.001 and that of loss is ∼10^{-4}. The dielectric breakdown strength of all the glasses was determined at room temperature in air medium using a high a.c. voltage breakdown tester (ITL Model AAH-55, Hyderabad) operated with an input voltage of 250 V at a frequency of 50 Hz; it was ensured that all the glasses used for this study were of nearly identical thicknesses. The magnetic susceptibility measurements were made by Guoy's method to an accuracy of 10^{-4} emu.

3. Results

The samples prepared were free from visible inhomogeneities, such as inclusions, cracks or bubbles. Based upon the visual examination, the absence of peaks in the X-ray diffraction pattern, SEM images, the existence of glass transition temperature T_g, we could come to the conclusion that the samples prepared were amorphous in nature. From the measured values of density d and calculated average molecular weight $\overline{M}$, various physical parameters such as silver ion concentration N_i, mean silver ion separation r_i, polaron radius r_p, which are useful for understanding the physical properties of these glasses are evaluated and presented in Table 1. The density of the glass is observed to increase with increase in the concentration of Ag_2O. The increase in the density although small is believed to be due to the replacement of lighter iron ions with the heavier silver ions in the glass matrix.

The dissolution rate of the lithium-iron phosphate glasses in distilled water solution (of pH 7) at 90 °C varied significantly with Fe_2O_3/Ag_2O content, as shown in Figure 2 and Table 1. The dissolution rate, decreased from 5×10^{-7} to 10^{-9} g·cm^{-2}·min^{-1} with an upward kink at 1.0 mol% of Ag_2O. The pH of the distilled water solution after corrosion testing shows a slow increase with increase in the concentration of Ag_2O from 0 to 0.6 mol% and from 1 to 1.5 mol%; however, a considerable decrease within the concentration range 0.8 to 1.0 mol% of Ag_2O and 4.2 to 4 mol% Fe_2O_3 (Figure 3) has been observed. Nevertheless, no significant change is observed, in pH of the liquid in contact with glasses containing 1.5 to 2.0 mol% of Ag_2O. The reduction in pH of the liquid in contact with glasses AF_8 and AF_{10} is consistent with the dissolution of phosphate species from these glasses and the subsequent formation of phosphoric acid.

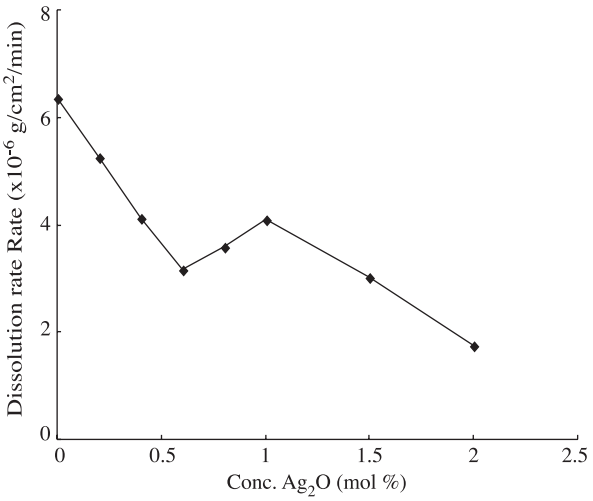

Figure 2. Dissolution rate of the lithium-iron phosphate glasses in distilled water solution at 90 °C.

Table 1. Various physical parameters of Li_2O–Fe_2O_3–P_2O_5 glasses doped with Ag_2O.

Glass	Density g·cm^{-3}	Average molecular weight	Conc. Ag^+ ions N_i (×10^{21} ion·cm^{-3})	Inter ionic distance r_i of Ag^+ ions (Å)	Polaron Radius r_p (Å)	Average Dissolution Rate (×10^{-7} g·cm^{-2}·min^{-1})
AF_0	2.3817	98.00	-	-	-	2.36
AF_2	2.3855	98.14	2.93	6.99	2.82	2.17
AF_4	2.3893	98.29	5.86	5.55	2.24	1.12
AF_6	2.3931	98.43	8.79	4.85	1.95	0.16
AF_8	2.3969	98.58	11.72	4.41	1.77	2.58
AF_{10}	2.4007	98.72	14.65	4.09	1.65	3. 02
AF_{15}	2.4102	99.08	21.98	3.57	1.44	0.14
AF_{20}	2.4197	99.44	29.31	3.24	1.31	0.02

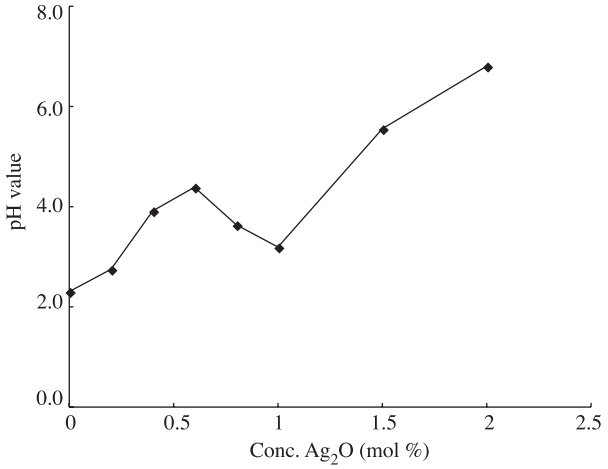

Figure 3. Variation of solution pH with the concentration of Ag_2O, after corrosion testing.

The infrared transmission spectra of Li_2O–Fe_2O_3–P_2O_5 glasses (Figure 4) exhibit vibrational bands around 1300 cm^{-1}, (identified due to anti-symmetrical vibrations of PO_2^- groups, this region may also consist of bands due to P=O stretching vibrations); 1050 cm^{-1} (arising out of symmetric stretching vibrations of

PO_2^- and the bands due to symmetric stretching normal vibrational mode in PO_4^{3-} may also lie in this region); and two prominent bands at 780 cm^{-1} due to P–O–P symmetric stretching vibrations. This region may also consist of bands due to pyrophosphate groups ($P_2O_7^{4-}$); and at 900 cm^{-1}, due to P–O–P asymmetric stretching vibrations [12–14]. With the gradual introduction of Ag_2O up to 0.6 mol%, the following changes in the vibrational bands of phosphate groups have been observed: (i) a progressive increase in the intensity of the bands due toPO_2^- and PO_4^{3-}vibrational groups, accompanied by a shift towards slightly lower wave number has been observed. (ii) The band due to P–O–P asymmetric stretching vibrations is shifted towards higher wavenumber with a considerable decrease in the intensity. When the concentration of Ag_2O is raised from 1.0 to 2.0 mol%, a gradual decrease in the intensity of the bands due to symmetrical stretching vibrational bands of phosphate groups is observed. Additionally, the spectra of these glasses have exhibited two FeO_6 octahedral bands due to ν_1 and ν_3 vibrations at 580 and 470 cm^{-1}, respectively [15, 16]. The spectra of these glasses have also exhibited a band at about 630 cm^{-1} identified due to the vibrations of FeO_4 tertrahedra. As the concentration of Ag_2O is increased up to 0.6 mol%, the intensity of the octahedral bands is observed to decrease gradually where as that of the FeO_4 tetrahedral units, is observed to increase. However, in the concentration range of 0.8 to 1.0 mol% of Ag_2O, the octahedral bands seem to be dominant over the octahedral bands; and beyond this concentration range, the occupation of iron ions in tetrahedral positions seems to prevail over octahedral positions. The summary of the data on the positions of various bands of IR spectra is presented in Table 2.

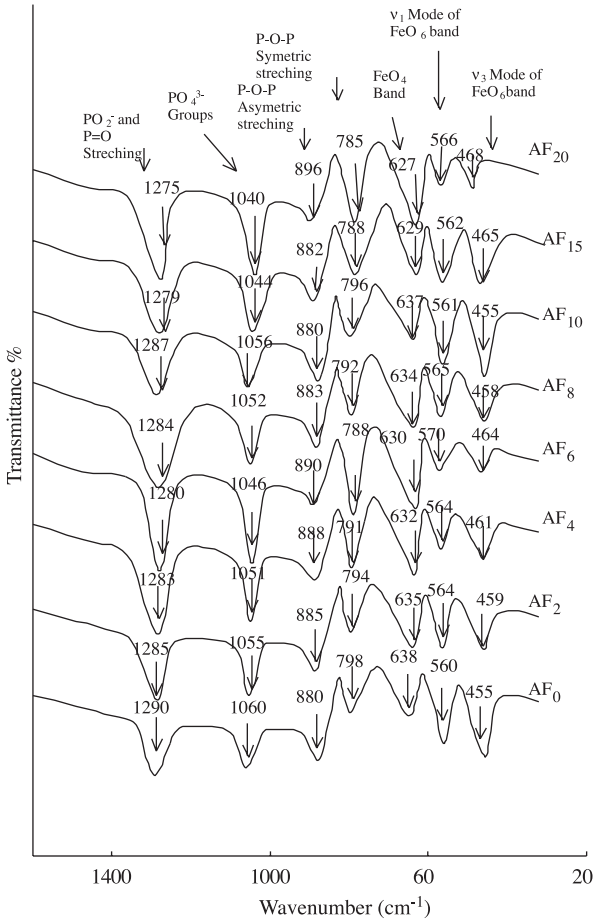

Figure 4. IR Spectra of Li_2O–P_2O_5–Fe_2O_3:Ag_2O glasses.

Table 2. Summary of the data on positions (cm^{-1}) of various absorption bands in the IR spectra of Li_2O–Fe_2O_3–P_2O_5:Ag_2O glasses.

	Glass AF_0	Glass AF_2	Glass AF_4	Glass AF_6	Glass AF_8	Glass AF_{10}	Glass AF_{15}	Glass AF_{20}
PO_2^- asymmetric groups (P=O stretching)	1290	1285	1283	1280	1284	1287	1279	1275
PO_4^{3-} groups	1060	1055	1050	1046	1052	1056	1044	1040
P−O−P Asymmetric stretching	880	885	888	890	883	880	882	896
P−O−P symmetric stretching	798	794	791	788	792	796	788	785
FeO_4 tetrahedra	638	635	632	630	634	637	629	627
ν_1-mode of FeO_6 octahedra	560	564	567	570	565	561	562	566
ν_3-mode of FeO_6 octahedra	455	59	461	463	458	455	465	468

The optical absorption spectra of Li_2O–Fe_2O_3–P_2O_5:Ag_2O glasses recorded in the wavelength region 300–1200 nm are shown in Figure 5a. The absorption edge observed at 343 nm for silver free glass is found to be shifted to slightly lower wavelength with increase in concentration of Ag_2O up to 0.6 mol%; whereas in the concentration range 0.8 to 1.0 mol% the edge is observed to shift towards higher wavelength. The absorption edge is observed at the lowest wavelength for the glass AF_{20}. From the observed absorption edges, we have evaluated the optical band gap E_o for each of these glasses by drawing a Urbach plot between $(\alpha\hbar\omega)^{1/2}$ and $\hbar\omega$ Figure 5b shows the Urbach plots of all these glasses in which a considerable part of each curve is observed to be linear. From the extrapolation of the linear portion of these curves, the values of optical band gap E_o are determined and presented in Table 3. The value of optical band gap is found to be the lowest for the glass AF_{10} and highest for the glass AF_{20}.

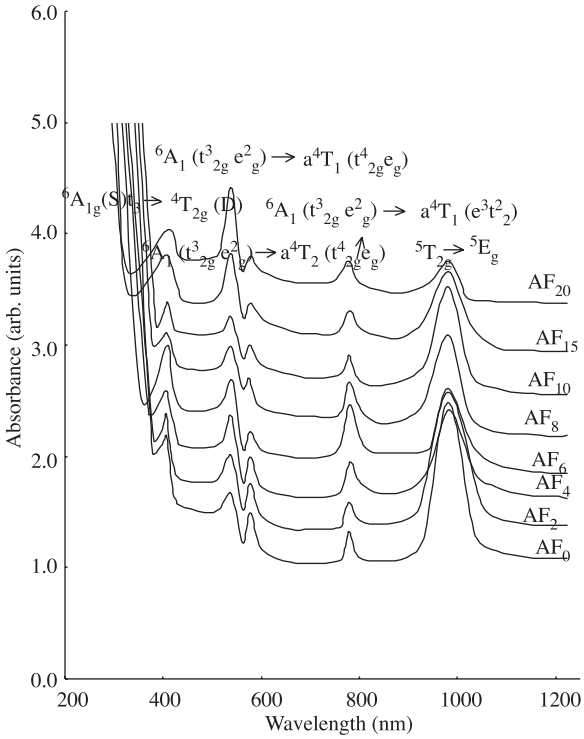

Figure 5a. Optical absorption spectra of Li_2O–P_2O_5–Fe_2O_3:Ag_2O glasses.

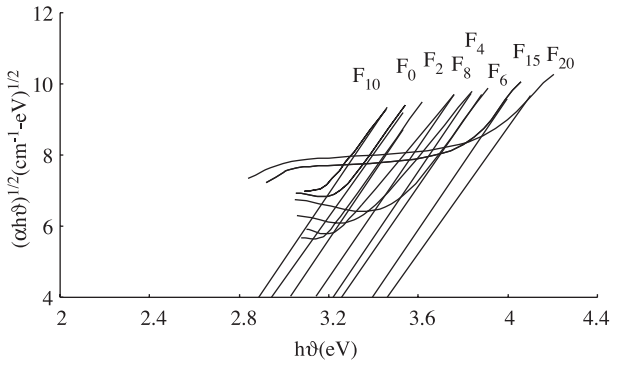

Figure 5b. Optical absorption spectra of Li_2O–P_2O_5–Fe_2O_3:Ag_2O glasses.

Table 3. Summary of data on optical absorption spectra of Li_2O–Fe_2O_3–P_2O_5:Ag_2O glasses.

Glass	Cut-off wavelength (nm)	Optical band gap E_0 (eV)
AF_0	343	2.90
AF_2	330	2.94
AF_4	323	3.16
AF_6	317	3.22
AF_8	350	3.06
AF_{10}	359	2.84
AF_{15}	306	3.32
AF_{20}	295	3.45

Furthermore, the spectra of all these glasses exhibited three absorption bands at 785, 580 and 540 nm, identified as due to transitions of Fe^{3+} ions [17]. Additionally, a band at 980 nm, identified as due to the transition of Fe^{2+} (d^6) ions [18], is also located in the spectra of all the glasses. With increase in the concentration of Ag_2O up to 0.6 mol%, the intensity of bands due to Fe^{3+} ions has been observed to increase; when the concentration of Ag_2O is raised beyond 0.6 mol%, a gradual decrease in the intensity of the bands due to Fe^{3+} ions could clearly be observed, while that of band due to Fe^{2+} ions is observed to increase; this trend continued to 1.0 mol%. Further increase of Fe_2O_3 was accompanied with an increase in intensity of the band due to Fe^{3+} ions. However, variation of Ag_2O concentration did not affect the band positions of iron ion transitions.

Magnetic susceptibility of Li_2O–Fe_2O_3–P_2O_5:Ag_2O glasses measured at room temperature is observed to increase with Fe_2O_3 content in the glass composition. From the values of magnetic susceptibilities, the effective magnetic moments μ_{eff} are evaluated and presented in Table 4. The value of μ_{eff} is found to lie in the region $5.6\mu_B$ to $5.7\mu_{Bg}$ for glasses AF_2 to AF_6, and AF_{15} to AF_{20} and decreases to within the range $4.3\mu_B$ –$4.4\mu_B$ for glasses AF_8 to AF_{10}.

ESR spectra for Li_2O–Fe_2O_3–P_2O_5:Ag_2O glasses were recorded at room temperature and are shown in Figure 6. The intense spectral line centred at about $g = 2.0$ can be clearly seen in the spectra of all the glasses. The intensity of this signal is observed to increase with the concentration of Ag_2O from 0.2 to 0.6 mol% and from 1.5 to 2.0 mol%; the signal however seemed to be weak in glasses AF_8 and AF_{10}. The value of g is found to be slightly higher for glasses AF_{15} and AF_{20} (see Table 4). Additionally, a weak signal at about $g = 4.3$ could be detected in the spectra of all the glasses.

Table 4. Data on magnetic susceptibility of Li_2O–Fe_2O_3–P_2O_5:Ag_2O glasses.

Glass	Magnetic susceptibility χ ($\times 10^{-6}$ emu)	μ (μ_B)	g
AF_0	5.7	16.19	1.99
AF_2	5.65	15.28	1.99
AF_4	5.6	14.38	1.99
AF_6	5.58	13.66	1.99
AF_8	4.4	8.11	1.99
AF_{10}	4.3	7.38	1.99
AF_{15}	5.71	11.39	2.02
AF_{20}	5.72	9.80	2.04

Dielectric constant ε' and loss tan δ at room temperature ($\approx$30 °C) of pure Li_2O–Fe_2O_3–P_2O_5 glasses at 100 kHz are measured to be 10.99 and 0.011, respectively. The values of these parameters are found to increase considerably with decrease in frequency. Figure 7 shows the variation of dielectric constant and loss of Li_2O–Fe_2O_3–P_2O_5 glasses containing different concentrations of Ag_2O with frequency, measured at room temperature. The values of ε' and tan δ are observed to slowly decrease with increasing concentration of Ag_2O, up to 0.6 mol%; and beyond this concentration (up to 1.0 mol %), these values are found to increase.

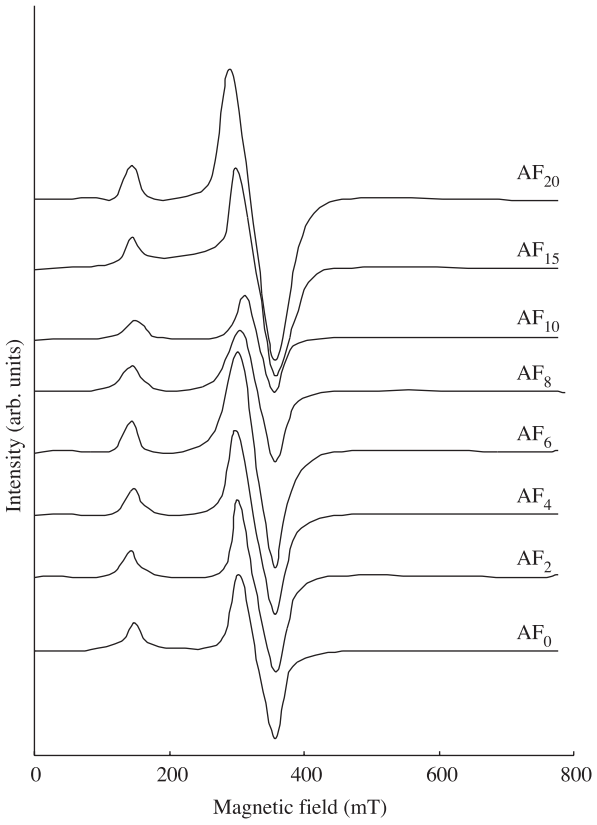

Figure 6. ESR spectra of Li_2O–P_2O_5–Fe_2O_3:Ag_2O glasses recorded at liquid nitrogen temperature.

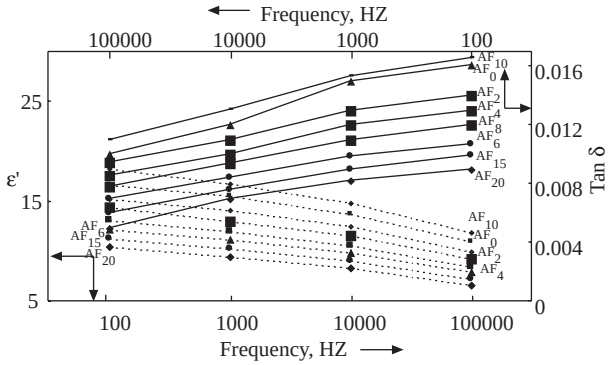

Figure 7. Variation of ε' and tan δ with frequency at room temperature of Li_2O–P_2O_5–Fe_2O_3 glasses doped with different concentrations of Ag_2O.

The temperature dependence of ε', for glasses containing different concentrations of Ag_2O at 1 kHz, is shown in Figure 8; and in the inset is shown ε' at different frequencies for glass AF_4. The value of ε' is found to exhibit a considerable increase at higher temperatures, especially at lower frequencies. However, the rate of increase of ε' with temperature is found lowest for the glass containing 2.0 mol% of Ag_2O, AF_{20}, and highest for the glass containing 1.0 mol%, AF_{10}.

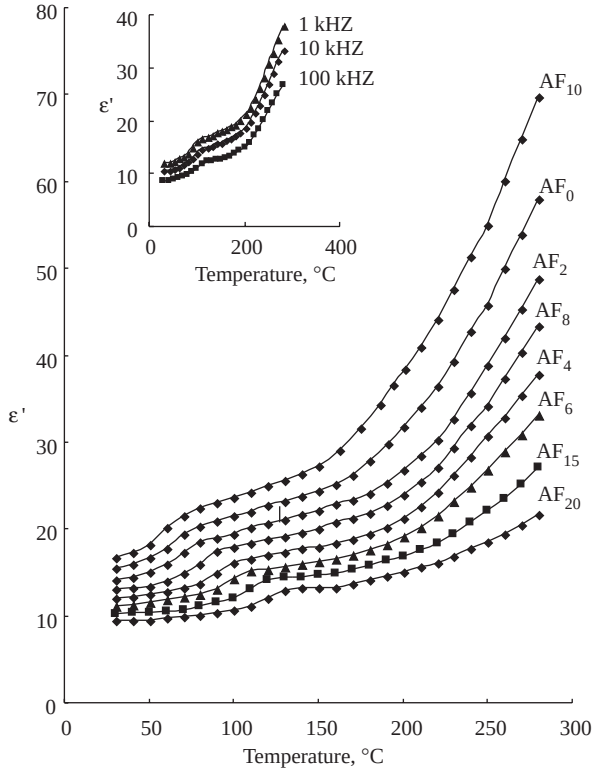

Figure 8. Plots comparing variation in dielectric constant with temperature at 1 kHz for Li_2O–P_2O_5–Fe_2O_3:Ag_2O glasses. Figure inset gives the variation of dielectric constant with temperature for glass AF_4 at different frequencies.

The temperature dependence of tan δ of all glasses measured at the frequency 10 kHz is presented in Figure 9. In the inset of the same figure is shown the variation of tan δ for glass AF_8, containing 0.8 mol% of Ag_2O, at different frequencies. The curves of both silver oxide-free and Ag_2O-doped glasses exhibited

distinct maxima, with the characteristic that, with increasing frequency, the temperature maximum shifts towards higher temperature and with increasing temperature the frequency maximum shifts towards higher frequency, indicating the dielectric relaxation character of dielectric losses of these glasses. Further, the observations on dielectric loss variation with temperature for different concentrations of Ag_2O show that the highest value of $(\tan\delta)_{\max}$ of relaxation curves for the glass AF_{10} and the lowest for the glass AF_{20}.

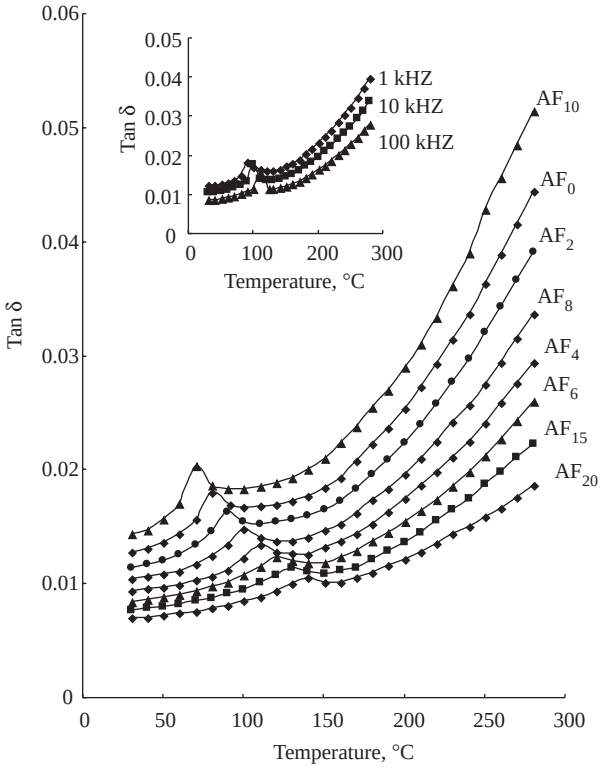

Figure 9. Plots comparing variation in dielectric loss with temperature for Li_2O–P_2O_5–Fe_2O_3:Ag_2O glasses at 10 kHz. Figure inset gives the variation of dielectric loss with temperature for glass AF_8 at different frequencies.

Using the relation

$$f = f_o \exp(-W_d/KT), \tag{1}$$

the effective activation energy W_d for the dipoles is calculated for different concentrations of Ag_2O and is presented in Table 5. The activation energy is found to increase with increase in the concentration of Ag_2O up to 0.6 mol%, and beyond this, up to 1.0 mol% of Ag_2O, the value of activation energy is found to decrease.

The a.c. conductivity as a function of frequency σ_{ac} is calculated using the equation

$$\sigma_{ac} = \omega\,\varepsilon'\varepsilon_\circ\, tan\,\delta, \tag{2}$$

where $\varepsilon_\circ$ is the vacuum dielectric constant. In Figure 10, $\log\sigma_{ac}$ is plotted against $1/T$ for glass AF_{10}, and $\log\sigma(1/T)$ is plotted for all glasses, at 10 kHz, in Figure 11. The conductivity is found to decrease considerably with increase in concentration of Ag_2O at any given frequency and temperature from 0 to 0.6 mol% (characterized in Figure 12). Note between 0.6 to 1.0 mol% the clear presence of a hike in the conductivity. From these plots, the activation energy for the conduction in the high temperature region over

which a near linear dependence of log σ_{ac} with $1/T$ could be observed is evaluated and its variation with the concentration of Ag_2O is shown in inset (a) of Figure 12.

Table 5. Data on dielectric loss of Li2O–Fe_2O_3–P_2O_5:Ag_2O glasses.

Glass	Average Tan δ_{max}	Temperature region of relaxation (°C)	Dipole Activation Energy (eV)
AF_0	0.0542	64–90	2.51
AF_2	0.0496	76–100	2.65
AF_4	0.0409	95–122	2.95
AF_6	0.0377	108–131	3.10
AF_8	0.0457	85–112	2.80
AF_{10}	0.0611	62–84	2.37
AF_{15}	0.0344	120–150	3.26
AF_{20}	0.0319	132–152	3.42

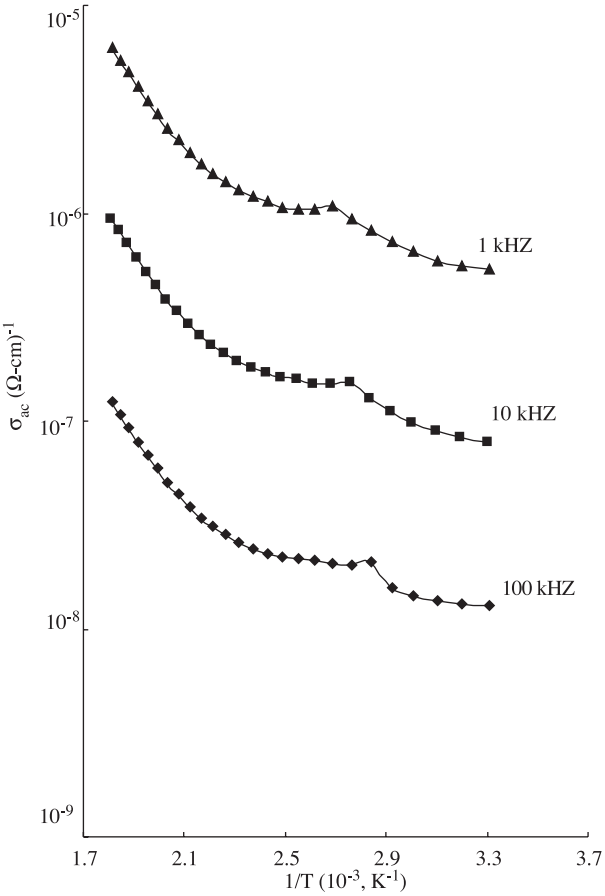

Figure 10. Variation of σ_{ac} with $1/T$ for glass AF_{10} at different frequencies.

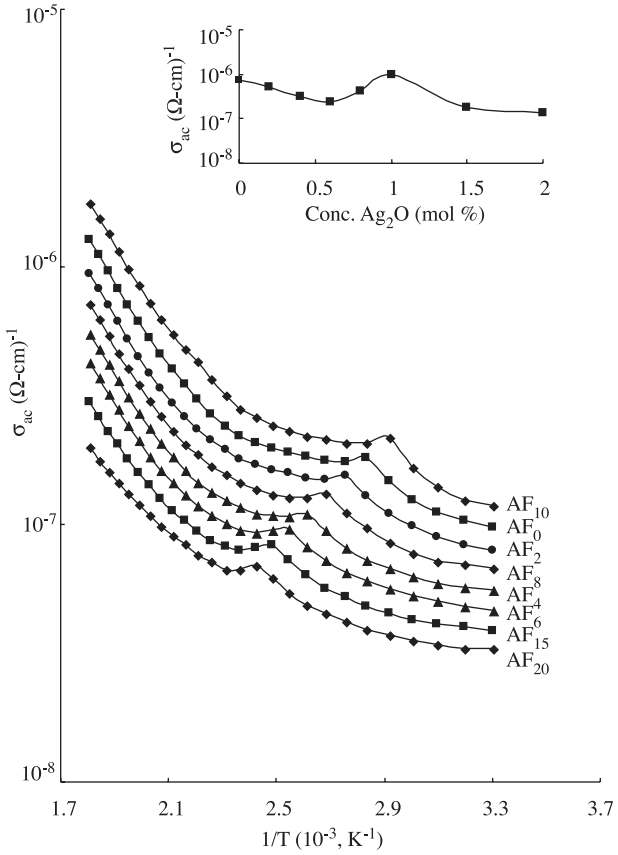

Figure 11. Plots comparing variation of a.c. conductivity with $1/T$ at 10 kHz for Li_2O–P_2O_5–Fe_2O_3:Ag_2O glasses. Inset gives the variation of σ_{ac} (at 240 °C and 10 kHz) with the concentration of Ag_2O.

4. Discussion

Li_2O–P_2O_5–Fe_2O_3:Ag_2O glasses have a complex composition and are an admixture of network formers and modifiers. Normally the structure of the simple phosphate glasses is dependent on O/P ratios and the fraction of Q phosphate tetrahedra. For single P_2O_5 glass O/P = 2.5 and the glass network is build up of Q^3 tetrahedra with the bridging oxygens; and with the fourth oxygen, is doubly bonded to the phosphorus atom. With the addition of iron oxide an ultraphosphate network consisting of Q^2 and Q^3 tetrahedra may form with O/P < 3.0 [19].

Li_2O and Ag_2O are well known modifier oxides and enter the glass network either by rupturing or by breaking up the P–O–P structures. (Normally, the oxygens of M_2O break the local symmetry, while the M^+ ions occupy interstitial positions.) In turn, the breakup of the P–O–P structures introduce coordinated defects, known as dangling bonds, along with non-bridging oxygen ions. Iron may exist both in Fe^{2+} and Fe^{3+} states.

The speciation of iron in these glasses is controlled by the reversible reaction

$$4Fe^{3+}_{\text{melt}} + 2O^{2-}_{\text{melt}} \rightleftharpoons 4Fe^{2+}_{\text{melt}} + 2O_{2\ \text{meltatm}}.$$

where 'melt atm' stands for melting in a reducing atmosphere.

Fe^{3+} ions are expected to occupy both tetrahedral and octahedral positions in the glass network. However, the four-fold coordination of Fe^{3+} is observed to be more common than the six fold coordination in many of the glasses [20]. Both of these Fe^{3+} sites can be considered as substitutional and subjected to strong

interaction between its external orbitals and the p-orbitals of the neighbouring oxygens [21] and form the linkages of the type P–O–Fe. Basing on the above discussion, the anticipated structure of Li_2O–Fe_2O_3–P_2O_5:Ag_2O glass network is illustrated in Figure 13.

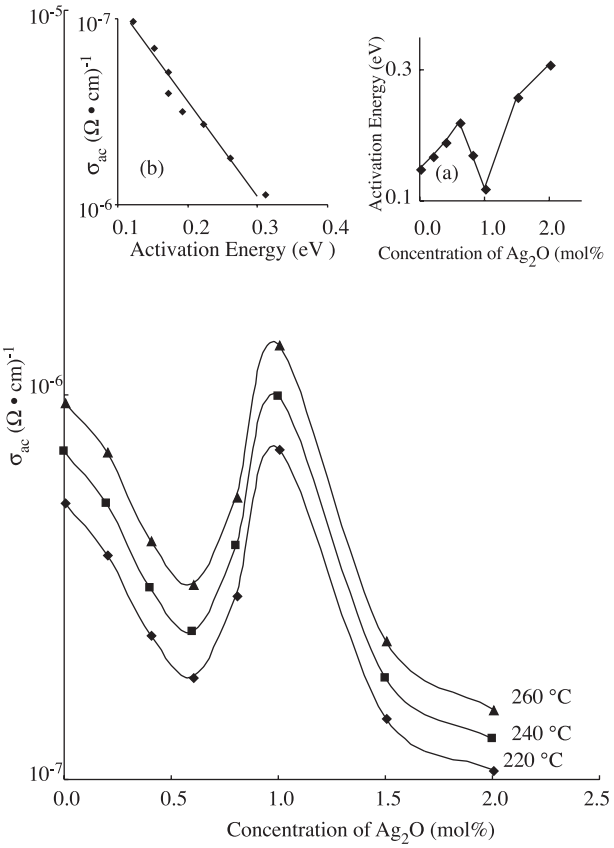

Figure 12. A.C. conductivity isotherms, at 10 kHz, of Li2O–P_2O_5–Fe_2O_3 glasses, as a function of Ag_2O concentation. Inset (a) shows the variation of activation energy for conduction, as a function of Ag_2O concentration; and inset (b) gives the variation of conductivity as a function of activation energy.

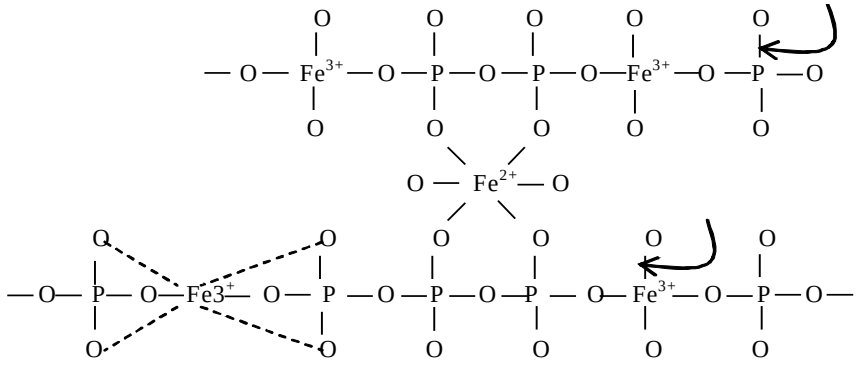

Figure 13. An illustration of Li_2O–Fe_2O_3–P_2O_5: Ag_2O glass network with Fe^{3+} ions in both tetrahedral and octahedral substitutional positions and Fe^{2+} in octahedral positions. Arrow indicates the entry of modifier ions (Li^+, Ag^+).

Fe^{2+} ions are expected to occupy only interstitial positions since the ratio of cation-oxygen radii is 0.63 for Fe^{2+} ion, which is far from the value of 0.19 possessed by an ion to occupy tetrahedral or substitutional sites [21] and act as modifiers similar to Li^+ and Ag^+ ions.

The ingress of Ag^+ ions may result in the following changes in the glass network. The P–O–Fe linkages are expected to form from P–O–P and Fe–O–Fe complexes. After the entry of Ag^+ ions, these linkages may be modified as per the following relations:

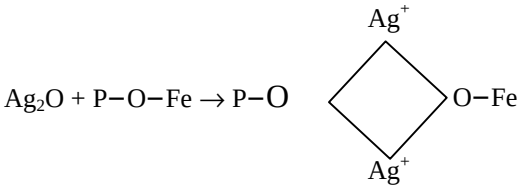

or,

P–O–Fe + Ag_2O → P–O^-Ag^+ + Fe–O^-Ag^+.

As a consequence there is a disruption in the PO_4 and FeO_4 tetrahedral with the creation of number of non-bridging oxygens.

The dissolution rate of Li_2O–Fe_2O_3–P_2O_5:Ag_2O glasses in water at 90 °C varied considerably with the change in the concentration of Fe_2O_3 or Ag_2O in the glass matrix. Glasses containing 0.6 to 1.0 mol% Ag_2O have a significant dissolution rate when compared with that of other glasses; further, the external surface of these glasses was observed to be rough and heavily pitted after corrosion testing. On the other hand, glasses AF_{15} and AF_{20} showed a remarkable improvement of chemical durability; surfaces of these samples after the testing are observed to be smooth, with the corners and the edges retaining original sharpness. The pH of the residual water solution also correlates notable improvement of the durability of glasses AF_{15} and AF_{20}. The observed decrease in the average dissolution rate (DR) of the glasses with increase in the concentration of Ag_2O indicates that the concentration of undisturbed P–O–P and P–O–Fe bonds is higher in the glasses containing 0.6 mol% and 2.0 mol% of Ag_2O. This is also an indication of a high Fe:P ratio (yet with value <1, for substitutionally positioned Fe) in these glasses. The presence of such unruffled bonds at higher concentrations makes the glasses more corrosion resistant. Additionally, the length and orientation distribution of PO_4 chains also play a major role in deciding the chemical durability of these glasses. Previous empirical studies showed that the shortened PO_4 chains in the glass network are responsible to some extent for the high corrosion resistance of the glasses [22]. This conclusion obviously suggests in this concentration ranges (4.4–5.0 and 3.0 to 3.5 mol%), the iron ions prefer to go in to the network forming positions rather than acting as modifiers and the role of Ag^+ ions as modifiers in this concentration range seems to be minimal. The considerable decrease observed in the pH value of the residual water solution with in the concentration range 0.8 to 1.0 mol% of Ag_2O or 4.2 to 4 mol% Fe_2O_3 (Figure 3b) clearly indicates that corrosion resistance in these glasses is comparatively low.

The optical absorption spectra of these glasses have exhibited four absorption bands at 408, 540, 580 and 785 nm. Using Tanabe-Sugano diagrams for d^5 ion, the spectra have been analyzed and the bands are assigned to $^6A_1$ (S)t_0 $\rightarrow{}^4T_2$ (D), $^6A_1(t_{2g}^3e_g^2)$ $\rightarrow$ $a^4T_1(t_{2g}^4e_g)$, $^6A_1(t_{2g}^3e_g^2)$ $\rightarrow$ $a^4T_2(t_{2g}^4e_g)$, $^6A_1(e^2t_2^3)$ $\rightarrow$ $a^4T_1(e^3t_2^2)$ (spin forbidden) transitions of Fe^{3+} ions, respectively [24] with LF parameters, Dq (crystal field splitting energy) =1282 cm^{-1} and Racah inter electronic repulsion parameters B = 840 cm^{-1}. More precisely, basing on selection rules and ligand field calculations, the band $^6A_1$ $(e^2t_2^3)$ $\rightarrow$ a^4T_1 $(e^3t_2^2)$ is identified due to FeO_4 groups, and the remainder due to FeO_6 groups. The band observed at 977 nm is identified due to $^5T_{2g}$ $\rightarrow{}^5E_g$ transition of Fe^{2+} (d^6) ions [23].

The observed increase in the intensity of Fe^{3+} ion bands up to 0.6 mol%, and from 0.8 mol% of Ag_2O, indicates that in this concentration range the silver ions facilitate Fe^{3+} ions to occupy substitutional positions. When the concentration of Fe_2O_3 is raised from 0.6 to 1.0 mol%, the $^5T_{2g}$ $\rightarrow{}^5E_g$ transition of Fe^{2+} ions

(d^6) seems to be dominant over the transitions from $^6A_1$ ground state, indicating that in this concentration range, the iron ions predominantly exist in divalent state and occupy only interstitial positions [23].

Increase in concentration of modifying ions that participate in the depolymerisation of the glass network leads to a decrease in the concentration of bonding defects and non-bridging oxygens (NBO). Higher the concentration of such modifiers, higher is the concentration of NBOs in the glass matrix. This leads to an increase in degree of localization of electrons by increasing the donor centres in the glass matrix. The increasing presence of these donor centres decreases the optical band gap and shifts the absorption edge towards higher wavelengths. The decrease in the optical band gap E_o with increase in the concentration of Ag_2O from 0.6 to 1.0 mol% (Table 3) obviously indicates an increasing degree of depolymerisation of the glass network, where as higher values of E_o for the glasses AF_{15} and AF_{20} suggest high rigidity of these glasses. It may be worth mentioning that the IR spectra of these glasses appear dominated by orthophosphate structural units; however, the band due to pyrophosphate structural units lies around 1090 cm^{-1}, which is not too far from the band position of PO_4^{3-} units. Hence the observed band at about 1090 cm^{-1} in the spectra of these glasses may indicate the superposition of these two bands, especially in the spectrum of more disordered glass. The same is true for metaphosphate groups also, because the band due to these groups is expected at about 1280 cm^{-1} [24].

If silver and divalent iron ions act as modifiers, the π-bond of P=O may be ruptured, creating new non-bridging oxygens. Even if Fe^{3+} ions enter substitutional positions with octahedral units in the glass network, the PO_4 structural units are subjected to perturbations (like bonding, compression and chemical interactions) due to change in the environment and the incompatibility in ion size. As a result, PO_4 structural units undergo structural distortions involving changes in bond lengths and angles of P–O bonds. For these reasons we expect decrease in the intensity of the bands due to PO_2^- stretching vibration, PO_4^{3-}symmetric stretching and a band due to P-O-P symmetric/ Fe–O–P stretching vibrations in the IR spectra. The observed gradual decrease in the intensity of these bands in the spectra of the glasses AF_8 to AF_{10} may be ascribed to these reasons. The observed increase in the intensity of these symmetrical bands and simultaneous decrease in the intensity of the bands due to P–O–P asymmetric vibrations in the spectra of the glasses AF_{15} to AF_{20} suggests that, in the networks of these glasses, the iron ions mostly occupy tetrahedral positions and are less disturbed by silver ions.

The magnetic properties of these glasses arise from the $3d^5$ and $3d^6$ electrons of Fe^{3+} and Fe^{2+} ions, respectively. The value of the effective magnetic moment ($\sim$5.6 to 5.7 μ_B) obtained for glasses AF_{15} to AF_{20} confirms the highest concentration of Fe^{3+} ions in these glasses. The decrease in the value of μ_{eff} from $5.7\mu_B$ to $4.3\mu_B$ (for the glasses AF_8 and AF_{10}) indicates a gradual conversion of iron ions from Fe^{3+} state to Fe^{2+} state, that takes modifying positions and increase the degree of disorder in the glass network.

The ESR spectra of these glasses have exhibited two signals centered at $g = 4.3$ and 2.0. These two resonance lines have been discussed at length by many investigators [25, 26]. The absorption at $g = 4.2$ arises from tetrahedral environment and the line at $g = 2.0$ is predicted due on the Fe^{3+}–O–Fe^{3+} spin pair [27]. However, there are reports suggesting that the $g = 4.3$ line arises due to rhombic sites of either tetrahedral or octahedral coordination [28]. Since, it is also evident from the IR spectra that the band due to FeO_4 units is more intense for glass AF_{20}, the relatively high intensity of the ESR signal observed for the same glass reinforces the view that the majority of the iron ions in the glass AF_{20} occupy tetrahedral positions.

Since Fe^{3+} ion belongs to d^5 configuration with ^6S ground state there is no spin-orbit coupling. As a result we expect that the value of g very near to free ion g value, i.e. 2.0023. However for the present glasses, we have observed values of g greater than 2.0 for glasses AF_{15} and AF_{20}. Such higher values of g arise when certain symmetry elements are present. The spin Hamiltonian associated with such higher values of g is usually expressed as [29]

$$H = g\beta BS + D[S_z^2 - \{S(S+1)/3\}] + E(S_x^2 - S_y^2), \tag{3}$$

where $S = 5/2$. Here, D and E are the axial and rhombic structure parameters and $\lambda = E/D$ lies within the limits $0 \leq \lambda \leq \frac{1}{3}$.

The $^6S_{5/2}$ ground state of Fe^{3+} (d^5) free ion is expected to split in to three Kramers doublets $|\pm 5/2\rangle$, $|\pm 3/2\rangle$ and $|\pm 1/2\rangle$ with separation normally greater than the microwave quantum. The symmetric and isotropic line observed at $g = 4.3$ in the present glasses is due to the middle Kramers doublets containing an admixture of different $|\pm m_j\rangle$ which are identified due to the low symmetry term $E(S_x^2 - S_y^2)$ in the Hamiltonian, the signal with $g = 2.0$ is due to EPR transitions in the $|\pm 1/2\rangle$ doublet [30].

The effective value of g obtained from ESR spectra show a gradual increase from 1.99 (Table 5) with increase in the concentration of Ag_2O in the glass matrix from 1.0 to 2.0 mol%. This is partly ascribable to the contribution of orbital angular momentum to the magnetic moment of Fe^{3+} ions. The fraction of the magnetic moment due to the orbital angular momentum I_s (orb), to that due to spin angular momentum, I_s (spin), may be expressed as [31]

$$I_s/I_o = (g/2) - 1. \tag{4}$$

Such an interesting feature may be understood in terms of the dipolar interactions, which are more predominant in the glass with the content of Fe_2O_3; these interactions cause a localized magnetic field at the site of Fe^{3+} ion and increase the effective g value, as observed [32].

The observed low intensity of the ESR signal in the concentration range of 0.8 to 1.0 mol % of Ag_2O (Fig. 6), may be due to both the destruction of more Fe^{3+}–O–Fe^{3+} pairs than are formed Fe–O^-Ag^+ complexes; and the reduction of Fe^{3+} iron ions to Fe^{2+}. This is also evidenced from optical absorption spectra (Fig. 5a); the spectra show a gradual growth of the band due to Fe^{2+} ions (i.e., $^5T_{2g} \rightarrow {}^5E_g$ band) at the expense of the bands due to Fe^{3+} ions with in this concentration range of Fe_2O_3.

Usually, electronic, ionic, dipolar and space charge polarizations contribute to the dielectric constant; among these, the space charge polarization depends on the perfection of the glass network. Normally, the modifying ions generate bonding defects in the glass network; these defects create easy path ways for the migration of charges that would build up space charge polarization and lead to an increase in the dielectric parameters [33–35].

The data on the dielectric properties of Li_2O–Fe_2O_3–P_2O_5:Ag_2O glasses show a gradual decrease in the parameters dielectric constant ε', loss tan δ and a.c. conductivity σ_{ac}, with increase in the concentration of Ag_2O in the glass network, from 1.0 to 2.0 mol%. These results suggest that there is a decrease in the concentration of free charge carriers that build up space-charge polarization [36, 37]. This observation supports the view point that in the glasses AF_{15} to AF_{20}, iron ions participate in the network forming with FeO_4 tetrahedral units. The gradual increase of these parameters with increasing content of Ag_2O from 0.6 to 1.0 mol%, suggests a greater degree of disorder in the glass network that enhances space charge polarization. In other words, in this concentration range the iron ions mostly occupy octahedral positions and disrupt the glass network similar to Li^+ and Ag^+ ions.

The observed dielectric relaxation effects may be attributed to association of divalent iron, Fe^{2+} ions, with a pair of PO_2^- groups in analogy with the mechanism-association of divalent positive ion with a pair of cationic vacancies in conventional glasses, glass ceramics and crystals [38, 39]. The lower values of tan δ_{max} and the higher values of activation energy for dipoles for the glasses AF_{15} and AF_{20} suggests a decreasing degree of freedom for dipoles to orient in the field direction in the networks of these glasses. Indirectly, it leads to the conclusion that there is an increasing stiffness of the glass network as the concentration of Ag_2O is increased from 1.0 to 2.0 mol%.

When log $\sigma(\omega)$ is plotted as a function of activation energy for conduction (in the high temperature region) a near linear relationship is observed (see inset (b) of Figure 12). This observation suggests that the conductivity enhancement is directly related to the thermally stimulated mobility of the charge carriers in the high temperature region [40].

The conductivity curve as a function of Ag_2O concentration passes through a maximum at $x = 1.0$ mol% (Figure 12). The activation energy for conduction as a function of the concentration of Ag_2O, exhibited

a minimum $x = 1.0$ mol% (see inset (a) of Figure 12). Thus Figure 12 and its insets suggest a kind of transition from predominantly electronic (zone-I, for $0.6 < x < 1.0$ mol%) to electric (zone-II for $x > 1.0$ mol%) conductivity [41]. The mobile electrons, or polarons, involved in the process of transfer from Fe^{3+} to Fe^{2+}, are attracted by the oppositely charged Ag^+ and/or Li^+ ions. This cation-polaron pair moves together as a neutral entity. As expected, the migration of this pair is not associated with any net displacement of the charge and thus does not contribute to electrical conductivity. As a result, we expect a decrease in the conductivity, as observed in zone-II [42]. In other words, with the entry of Ag^+ ions into the glass network, the electronic paths are progressively blocked causing an inhibition of the electronic current with a simultaneous increase in the ionic transport of Ag^+.

The value of $N(E_F)$, the density of the defect energy states (in the nearly temperature independent part of the conductivity range), is evaluated using the equation [43-46]

$\sigma o \omega pg = g(\pi vzpg^2 KT\ [\ N(E_F)\ ]^2 \alpha^{-5} \omega\ [\ \ln(\nu_{ph}/\omega)\ ]^4$, (5)

at frequency $\omega = 10^4$ Hz at $T = 340$ K, taking $\alpha = 0.50\ \mathring{A}^{-1}$ (electronic wave function decay constant, obtained by plotting log σ_{ac} against R_i) and $\nu_{ph} \sim 5{\times}10^{12}$ Hz; the results are presented in Table 6. The value of $N(E_F)$ is found to decrease with increasing concentration of Fe_2O_3up to $x = 0.6$ mol% (indicating decreasing disorder in the glass network); and thereafter, $N(E_F)$ is observed to increase (see Table 6).

Table 6. The concentration of defective energy states and a.c. conductivity of Li_2O–CaF_2–P_2O_5:Ag_2O glasses.

Glass	$N(E_F)$ ($\times 10^{20}$ $eV^{-1}{\cdot}cm^{-3}$)	Activation Energy (eV)
AF_0	7.83	0.15
AF_2	6.80	0.17
AF_4	5.30	0.19
AF_6	4.85	0.22
AF_8	5.98	0.169
AF_{10}	9.56	0.12
AF_{15}	4.34	0.26
AF_{20}	3.93	0.31

When the dielectric is placed in an electric field, the heat is liberated due to dielectric loss. If the applied field is an alternating field, the specific dielectric loss, i.e., the loss per unit volume of the dielectric is given by

$$\rho_1 = E^2 \omega \varepsilon' \varepsilon_\circ \tan\delta \quad W \cdot m^{-3}. \tag{5}$$

This equation indicates that, the lower the values of $\varepsilon' \tan\delta$ for the glass at a given frequency, are the values of ρ_l. The dielectric breakdown strength, on the other hand, is in fact inversely proportional to the specific dielectric loss represented by equation (6). Our observations on dielectric parameters of Li_2O–Fe_2O_3–P_2O_5:Ag_2O glasses, as mentioned earlier, indicate, the rate of increase of $\varepsilon' \tan\delta$ with temperature is the highest for glass AF_{10} and the lowest for the glass AF_{20}. Thus the experiments on dielectric properties of Li_2O–Fe_2O_3–P_2O_5:Ag_2O glasses also reveal that there is an increase in the dielectric breakdown strength of the glasses with increase in the concentration of Ag_2O beyond 1.0 mol%. This revelation is also consistent with the view that, in the concentration range of 1.5 to 2.0 mol%, the iron ions mostly exists in trivalent state and occupy network forming positions with FeO_4 structural units and increase the rigidity of the glass network.

5. Conclusions

The summary of the results of various studies of Li_2O–Fe_2O_3–P_2O_5 glasses doped with different concentrations of Ag_2O is as follows. The present analysis of chemical durability suggests that glasses containing Ag_2O above 1.0 mol% are more corrosion resistant. Optical absorption and magnetic susceptibility studies indicated that iron ions in these glasses exist both in trivalent and divalent states. IR spectral studies indicated that iron ions exist in tetrahedral and octahedral substitutional positions and form P-O-Fe linkages. The entry of Ag^+ ions causes formation of P–O^-Ag^+ and Fe–O^-Ag^+ complexes in the glass network. The results of dielectric properties indicate that the a.c. conduction, with in the concentration range of 0.6 to 1.0 mol% of Ag_2O, is mainly electronic in nature, whereas in the samples containing more than 1.0 mol% Ag_2O, ionic conduction seems to prevail.

Acknowledgements

One of the authors, K. Sambasiva Rao, is grateful to University Grants Commission, New Delhi for granting a fellowship under the Faculty Improvement Programme. He also wishes to thank the management of the J. K. C. College, Guntur for granting study leave.

References

[1] B. C. Sales and L. A. Boatner, *Science,* **226,** (1984), 45.

[2] Y. B. Peng and D. E Day, *Glass Technol.,* **32,** (1991), 166.

[3] B. V. R. Chowdari and P. Pramoda Kumari, *J. Phys. Chem. Sol.*, **58,** (1997), 515.

[4] J. E. Garbarczyk, P. Machowski, M. Wasiucionek, L. Tykarski, R. Bacewicz, A.Aleksiejuk, *Solid State Ionicks,* **136,** (2000), 1077.

[5] R. A Montani, A. Lorente, M. A Vincenzo, *Solid State Ionicks,* **130,** (2000), 91.

[6] N. H. Ray, *Br. Polym. J.,* **11,** (1979), 163.

[7] G. K. Marasinghe, M. Karabulut, C. S. Ray, D. E. Day, C. H. Booth, P. G. Allen, D. K. Shuh, *Ceram. Trans.*, **87,** (1998), 261. *J. Non-Cryst. Solids*, **249,** (1999), 261.

[8] Xiaoyan Yu, Delbert E. Day, Gary J. Long, Richard K. Brow, *J. Non-Cryst. Solids,* **215,** (1997), 21.

[9] Wen-Hai Huang, Nai Zhou, Delbert E. Day, Chandra S Ray, Xuebao Wuji Cailiao, *J. Inorg. Mater,* **20,** (2005), 842.

[10] A. Mogus-Milankovic, A. Santic, V. Licina and D. E. Day, *J. Non-Cryst. Solids*, **351,** (2005), 3235.

[11] A. Veerabhadra Rao, C. Laxmikanth, B. Apparao and N. Veeraiah, *J. Phys. Chem. Solids*, **67,** (2006), 2263. G. Naga Raju, N. Veeraiah**,** G. Nagarjuna, P. V. V. Satyanarayana, *Physica B Condensed Matter Phys*, **373,** (2006), 297.

[12] S. V. G. A. Prasad, G. S. Baskaran, N. Veeraiah, *Phys. Stat. Ssolidi a,* **202,** (2005), 2828.

[13] J. J. Hudgens and S. W. Martin, *J. Am. Ceram. Soc.*, **76,** (1994), 1691.

[14] K. Aomari, M. Saidi, and I. Drissi, *Phys. Chem. Glasses,* **38,** (1997), 15. **139**, (2006), 64*; Physica B*, **373,** (2006), 297.

[15] E. B. Araujo, J. A. Eiras, E. F.de. Almeida, J. A. C. de Paiva, and A. S. B. Sombra, *Phys. Chem. Glasses,* **40,** (1999), 273.

[16] G. Wang, Y. Wang, B. Jin, *SPIE,* **2287,** (1994), 214. Xiangyu Fang, Chandra S. Ray, Gaya K. Marasinghe, Delbert E. Day, *J. Non-Cryst. Sol.*, **263,** (2000), 293.

[17] E. Baiocchi., A. Montenero, M. Bettinelli, *J. Non-Cryst. Solids,* **46,** (1981), 203.

[18] F. Albert Cotton, G. Wilkinson, *Advanced Inorganic Chemistry*, (Wiley Eastern Ltd., New Delhi) 1976.

[19] M. Karabult, E. Metwalli, D. E. Day, R. K. Brow, *J. Non-Cryst. Solids,* **328,** (2003), 199.

[20] E. Baiocchi, A. Montenero, M. Bettinelli, *J. Non-Cryst. Solids,* **46,** (1981), 203.

[21] S. M. D. Nery, W. M. Pontuschka, S. Isotani, C. G. Rouse, *Phys. Rev.*, **49,** (1994), 3760.

[22] A. K. Varshneya, "Fundamentals of Inorganic Glasses", p. 35. Academic press, London, (1994).

[23] S. T. Reis, D. L. A. Faria, J. R. Martinelli, W. M. Pontuschka, D. E. Day, C. S. M. Partiti, *J. Non-Cryst. Solids,* **304,** (2002), 188.

[24] Xiangyu Fang, Chandra S. Ray, Andrea Mogus-Milankovic, Delbert E. Day, *J. Non-Cryst Solids,* **283,** (2001), 162.

[25] I. Ardelean, M. Toderas, S. Filip, *J. Mag. Magnetic Mater*, **272,** (2004), 339.

[26] D. Rusu, M. F. Carrasco, M. Toderas, I. Ardelean, *J. Mod. Phys B,* **19,** (2005), 1821.

[27] K. Tanaka, K. Kamiya, T. Yoko, *J. Non-Cryst. Solids*, **109,** (1989), 289.

[28] D. Loveridge, S. Parke, *Phys. Chem. Glasses,* **12,** (1971), 90.

[29] B. Bleaney, K. W. H. Stevens, *Rep. Prog. Phys.*, **16,** (1953), 108.

[30] A. Abragam, B. Bleaney, Electron paramagnetic resonance of transition ions, *Clarendon Press, Oxford*, 1970.

[31] J. H. Van Vleck, *Phys. Rev.*, **78,** (1950), 266.

[32] T. Komatsu, N. Soga, M. Kunugi, *J. Appl. Phys.*, **50,** (1979), 6469.

[33] M. Srinivasa Reddy, S. V. G. V. A. Prasad and N. Veeraiah, *Phy. Stat. Solidi* (a), **204,** (2006), 816.

[34] G. Murali Krishna and N. Veeraiah, N. Venkatramaiah and R. Venkatesan *J. Alloys Comp., DOI:10.1016/*j.jallcom.2006.10.148.

[35] M. Srinivasa Reddy, G. Naga Raju, G. Nagarjuna and N. Veeraiah, *J. Alloys Comp.*, DOI:10.1016/j.jallcom.2006.08.054.

[36] N. Krishna Mohan, K. Sambasiva Rao, Y. Gandhi, N. Veeraiah, *Physica B,* **389**, (2007), 213.

[37] A. Veerabhadra Rao, C. Laxmikanth and N. Veeraiah, *J. Phys. Chem. Solids*, **67,** (2006), 2263.

[38] S. Radha Krishnan, R. S. Srinivas Setty, *Phys. Rev.*, **14,** (1976), 969.

[39] N. Veeraiah, *J. Mater. Sci.*, **22,** (1987), 2017.

[40] G. El-Damarawi, *J. Phys. Condens. Matter,* **7,** (1995), 1557.

[41] R. A. Montani, M. A. Frechero, *Solid State Ionics,* **158,** (2003), 327.

[42] J. C. Bazan, J. A. Duffy, M. D. Ingram, M. R. Mallace, *Solid State Ionics*, **86,** (1996), 497.

[43] I. G. Austin, N. F. Mott, *Adv. Phys.*, **18,** (1969), 657.

[44] G. Naga Raju, and N. Veeraiah, *Physica B*, **373,** (2006), 297.

[45] G. Sahaya Baskaran, N. Krishna Mohan, V. Venkateswara Rao, D. Krishna Rao and N. Veeraiah, *Euro. Phy. J. Appl. Phys.*, **34,** (2006), 97.

[46] P. Nageswara Rao, B. V. Raghavaiah, D. Krishna Rao and N. Veeraiah, *J. Mater. Chem. Phys.*, **91,** (2005), 381.